J. Coat. Technol. Res., **9** (4) 483–493, 2012
DOI 10.1007/s11998-011-9379-1

The corrosion inhibition of maraging steel under weld aged condition by 1(2*E*)-1-(4-aminophenyl)-3-(2-thienyl)prop-2-en-1-one in 1.5 M hydrochloric acid medium

B. S. Sanatkumar, Jagannath Nayak, A. Nityananda Shetty

Abstract The influence of 1(2*E*)-1-(4-aminophenyl)-3-(2-thienyl)prop-2-en-1-one (ATPI) on the corrosion behavior of weld aged maraging steel in 1.5 M hydrochloric acid was studied by potentiodynamic polarization method and AC impedance (EIS) technique at different temperatures. The results showed that the inhibition efficiency of ATPI increased with the increase in the concentration of inhibitor and decreased with the increase in temperature. ATPI acts as a mixed type inhibitor without affecting the mechanism of the hydrogen evolution reaction or iron dissolution. The adsorption of ATPI on a weld aged maraging steel surface obeys the Langmuir adsorption isotherm equation. Both activation and thermodynamic parameters were calculated and discussed. ATPI inhibits the corrosion through both physisorption and chemisorption on the alloy surface. The surface morphology of the weld aged maraging steel specimens in the presence and the absence of the inhibitors was studied by the respective SEM images.

Keywords Maraging steel, ATPI, Corrosion rate, EIS, SEM

B. S. Sanatkumar, A. Nityananda Shetty (✉)
Department of Chemistry, National Institute of Technology Karnataka, Surathkal, Srinivasnagar 575 025, Karnataka, India
e-mail: nityashreya@gmail.com

J. Nayak
Department of Metallurgical and Materials Engineering, National Institute of Technology Karnataka, Surathkal, Srinivasnagar 575 025, Karnataka, India

Introduction

Corrosion inhibition of metals by organic compounds results from the adsorption of molecules and ions on the surface of the metals.[1–4] Several groups of organic compounds have been reported to exert inhibitive effects on the corrosion of steels. The extent of adsorption of an inhibitor depends on many factors such as the nature and the surface charge of the metal; the mode of adsorption of the inhibitor; the inhibitor's chemical structure; and the type of the aggressive solution. The presence of hetero atoms (oxygen, nitrogen, sulfur, and phosphorus), triple bonds, and aromatic rings in the inhibitor's chemical structure enhances the adsorption process. It has been reported that the order of the inhibitor efficiency (η) of heterocyclic organic compounds follows the sequence: oxygen < nitrogen < sulfur < phosphorus.[5–13]

Maraging steel is an important category of material due to its high technological value and wide range of industrial applications, especially in aerospace, automobile, and marine industries.[14–17] The alloy is a low carbon steel that classically contains about 18 wt% Ni, substantial amounts of Co and Mo, together with small additions of Ti. However, depending on the demands dedicated by the application, the composition of the material can be modified.[18] The high strength of maraging steel is achieved by aging at 480°C, where precipitation of intermetallics takes place. Because of the low carbon content, maraging steels have good machinability.[19] They have higher modulus of elasticity, lower thermal expansion coefficient, high strength, moderate toughness, and good weldability as compared with conventional alloy steels.[20] Another important property is its high thermal conductivity, which reduces surface temperature during thermal loading and lowers thermal stresses. Maraging steels are also used in preparation of surgical components, nuclear, and gas turbines applications.[14–17] Thus, they frequently come

into contact with acids during cleaning, pickling, descaling, acidizing, etc.

A search of the literature reveals only a few reports on the corrosion studies of 18 Ni 250 grade maraging steel, which is entirely in martensitic phase. Bellanger and Rameau[21] have studied the effect of slightly acidic pH with or without chloride ions in radioactive water on the corrosion of maraging steel and have reported that corrosion behavior of maraging steel at the corrosion potential depends on pH, and intermediates remaining on the maraging steel surface in the active region favoring the passivity. The effect of carbonate ions in a slightly alkaline medium on the corrosion of maraging steel was studied by Bellanger.[22] Maraging steels were found to be less susceptible to hydrogen embrittlement than common high-strength steels owing to significantly low diffusion of hydrogen in them.[23] Poornima et al.[17] have studied the corrosion behavior of 18 Ni 250 grade maraging steel in a phosphoric acid medium and reported that the corrosion rate of the annealed sample is less than that of the aged sample. Similar observations also have been reported for the corrosion of 18 Ni 250 grade maraging steel in sulfuric acid medium.[24] The effect of 3,4-dimethoxybenzaldehyde thiosemicarbazone in 0.5 M H_2SO_4 medium on corrosion of aged maraging steel was studied by Poornima et al.[25] and reported good inhibitor efficiency.

A few research reports revealed that the inhibition efficiency of chalcone derivatives is much higher than that of corresponding aldehydes and amines, and this may be due to the presence of a –C=C– group in the molecules and the presence of hetero atoms.[26,27] The planarity (π) and lone pairs of electrons present on hetero atoms are the important structural features that determine the adsorption of these molecules on the metal surface.

The objective of the present research article is to study the adsorption and inhibition action of synthesized ATPI on the corrosion of maraging steel under weld aged conditions in 1.5 M HCl medium at different temperatures using the potentiodynamic polarization method and the AC impedance (EIS) technique. The mode of adsorption and the corrosion inhibition mechanism are also discussed.

Experimental

Material

The material employed was 18% Ni M250 grade maraging steel under weld aged condition. The composition of the 18% Ni M250 grade maraging steel is given in Table 1. The maraging steel plates were welded by gas tungsten arc welding-direct-current straight polarity (GTAW-DCSP) using filler material of compositions 0.015% C, 17% Ni, 2.55% Mo, 12% Co, 0.015% Ti, 0.4% Al, 0.1% Mn, 0.1% Si, with the remainder being Fe. The specimen was taken from the plates which are welded as described above and aged at 480 ± 5°C for 3 h followed by air cooling.

Table 1: Composition of the aged maraging steel specimen

Element	Composition (wt%)	Element	Composition (wt%)
C	0.015	Ti	0.52
Ni	18.19	Al	0.11
Mo	4.82	Mn	0.1
Co	7.84	P	0.01
Si	0.1	S	0.01
O	30 ppm	N	30 ppm
H	2.0 ppm	Fe	Balance

Preparation of test coupons

Cylindrical test coupons were cut from the plate and sealed with epoxy resin in such a way that the area exposed to the medium was 0.64 cm^2. These coupons were polished mechanically using emery papers of grade nos. 180, 400, 600, 800, 1000, 1500, and 2000 and finally on a polishing wheel using legated alumina to obtain a mirror finish, washed thoroughly with double distilled water, and degreased with acetone before being immersed in the acid solution.

Medium

Standard solution of 1.5 M hydrochloric acid was prepared by diluting AR grade hydrochloric acid with double distilled water. Inhibitive action of ATPI on the corrosion of weld aged maraging steel in 1.5 M HCl solution was studied by introducing different concentrations of the inhibitor into the solution. The experiments were carried out at temperatures 30, 35, 40, 45, and 50°C (±0.5°C), in a calibrated thermostat.

Inhibitor

The inhibitor 1(2*E*)-1-(4-aminophenyl)-3-(2-thienyl) prop-2-en-1-one (ATPE) was synthesized as per the reported procedure[28] in one-step reaction of 4-aminoacetophenone (0.40 g, 3 mmol) with thiophene-2-carboxaldehyde (0.28 mL, 3 mmol) in ethanol (30 mL) in the presence of 10% NaOH (aq) (5 mL). The reaction mixture was stirred for 2 h at room temperature. The resulting yellow solid was collected by filtration, washed with distilled water, and dried. The product was purified by recrystallization from acetone and was identified by melting point (105–106°C), elemental analysis, and infrared spectra. The molecular weight of the compound is 229.29. The synthesis scheme is given below.

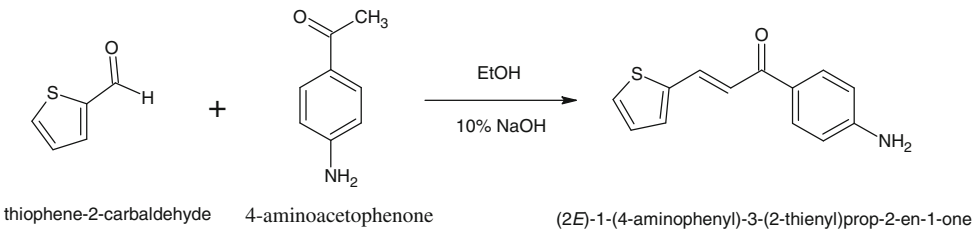

Electrochemical measurements

Electrochemical measurements were carried out by using an electrochemical work station, Gill AC having ACM instrument Version 5 software. The arrangement used was a conventional three-electrode compartment glass cell with a platinum counter electrode and a saturated calomel electrode (SCE) as reference. The working electrode was made of weld aged maraging steel. All the values of potential are referred to the SCE. The polarization studies were done immediately after the EIS studies on the same electrode without any further surface treatment.

Tafel polarization studies

Finely polished weld aged maraging steel specimen was exposed to the corrosion medium of 1.5 M hydrochloric acid in the presence and the absence of the inhibitor at different temperatures (30–50°C) and allowed to establish a steady-state open circuit potential (OCP). The potentiodynamic current–potential curves were recorded by polarizing the specimen to −250 mV cathodically and +250 mV anodically with respect to the OCP at a scan rate of 1 mV s^{-1}.

Electrochemical impedance spectroscopy studies (EIS)

The impedance measurements were carried out in the frequency range from 10 kHz to 0.01 Hz, at the rest potential, by applying 10 mV sine wave AC voltage. The double layer capacitance (C_{dl}) and the charge transfer resistance (R_{ct}) were calculated from the Nyquist plot.

In all the above measurements, at least three similar results were considered, and their average values are reported.

Scanning electron microscopy (SEM)

The surface morphology of the weld aged maraging steel specimen immersed in 1.5 M HCl solution in the presence and the absence of inhibitor was compared by recording the SEM images of the samples using JEOL JSM-6380LA analytical scanning electron microscopy. The immersion time of the electrode for the SEM analysis was 3 h.

Results and discussion

Tafel polarization measurement

The polarization studies of the weld aged maraging steel were carried out in 1.5 M hydrochloric acid solution containing different concentrations of ATPI at different temperatures using the Tafel polarization technique. Figure 1 shows the Tafel polarization curves for the corrosion of weld aged maraging steel in 1.5 M HCl solution at 45°C in the presence of different concentrations of ATPI. Similar results were obtained at other temperatures also. The inhibition efficiency, η (%), was calculated from the following equation (1).

$$\eta\,(\%) = \frac{i_{corr} - i_{corr(inh)}}{i_{corr}} \times 100 \qquad (1)$$

where i_{corr} and $i_{corr(inh)}$ are the corrosion current densities obtained in uninhibited and inhibited solutions, respectively. The corrosion rate is calculated using equation (2).

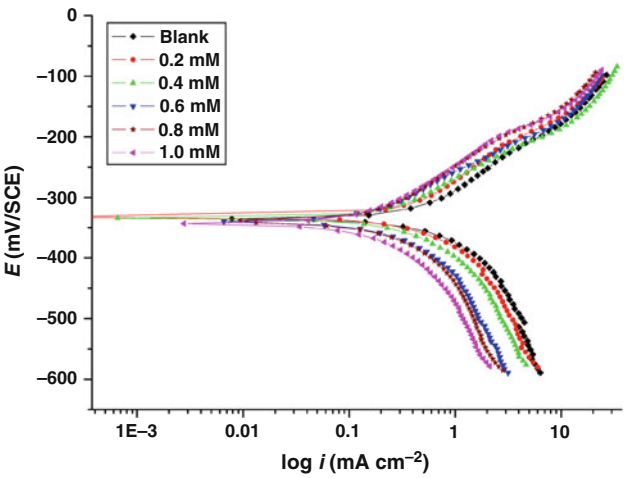

Fig. 1: Tafel polarization curves for the corrosion of weld aged maraging steel in 1.5 M hydrochloric acid containing different concentrations of inhibitor at 45°C

$$\upsilon_{corr}\ (\mathrm{mm\,y^{-1}}) = \frac{3270 \times M \times i_{corr}}{\rho \times Z} \quad (2)$$

where 3270 is a constant that defines the unit of corrosion rate, i_{corr} is the corrosion current density in A cm^{-2}, ρ is the density of the corroding material (g cm^{-3}), M is the atomic mass of the metal, and Z is the number of electrons transferred per atom.[29]

Corrosion parameters, such as corrosion potential (E_{corr}), cathodic and anodic Tafel slopes (b_c and b_a), corrosion current density (i_{corr}), and the inhibition efficiency values η (%), calculated from Tafel plots are listed in Table 2. As seen from the data, in the absence of inhibitor, weld aged maraging steel corrodes severely in 1.5 M HCl. The presence of inhibitor brings down the corrosion rate considerably. Polarization curves are shifted to a lower current density region indicating a decrease in corrosion rate (υ_{corr}). Inhibition efficiency increases with the increase in ATPI concentration. No definite trend is observed in the shift of E_{corr} values; both anodic and cathodic polarization profiles are influenced simultaneously, almost to the same extent, which indicate the influence of ATPI on both the anodic and the cathodic reactions; hydrogen evolution and metal dissolution.[30] If the displacement in corrosion potential is more than ±85 mV with respect to the corrosion potential of the blank, the inhibitor can be considered a distinctive cathodic or anodic type. However, the maximum displacement in this study is ±20 mV; and therefore ATPI can be considered a mixed-type inhibitor.[31,32]

The data in Table 2 show that there is no significant change in the values of cathodic Tafel slope b_c and anodic Tafel slope b_a with the increase in the concentration of the inhibitor. This suggests that the reduction mechanism at the cathode and the oxidation mechanism at the anode are not affected by the presence of inhibitor,[33,34] and hence the corrosion reaction is slowed down by the surface-blocking effect of the inhibitor. This indicates that the inhibitive action of ATPI may be considered due to the adsorption and formation of barrier film on the electrode surface. The

Table 2: Results of Tafel polarization studies on weld aged maraging steel in 1.5 M hydrochloric acid containing different concentrations of ATPI

Temperature (°C)	Conc. of inhibitor (mM)	E_{corr} (mV/SCE)	b_a (mV dec^{-1})	$-b_c$ (mV dec^{-1})	i_{corr} (mA cm^{-2})	υ_{corr} (mm y^{-1})	η (%)
30	Blank	−342	100	223	0.70	8.0	
	0.2	−339	102	221	0.39	4.2	47.8
	0.4	−345	105	215	0.28	3.1	61.1
	0.6	−343	103	213	0.21	2.2	73.0
	0.8	−348	104	209	0.85	1.1	86.0
	1.0	−351	107	210	0.08	0.8	90.2
35	Blank	−339	118	229	0.82	10.9	
	0.2	−342	115	226	0.59	6.2	43.1
	0.4	−338	112	222	0.44	4.5	58.7
	0.6	−344	108	219	0.34	3.6	67.5
	0.8	−347	111	217	0.20	2.1	80.6
	1.0	−343	106	215	0.13	1.5	87.0
40	Blank	−343	125	235	0.94	12.9	
	0.2	−337	127	233	0.72	7.5	42.0
	0.4	−340	121	228	0.53	5.7	55.6
	0.6	−342	119	230	0.41	4.4	65.7
	0.8	−341	115	225	0.26	2.9	77.7
	1.0	−336	109	221	0.18	1.9	84.8
45	Blank	−338	133	237	1.53	17.3	
	0.2	−335	135	233	0.90	10.7	38.2
	0.4	−337	129	235	0.79	8.2	52.6
	0.6	−339	126	228	0.64	6.9	60.1
	0.8	−341	123	225	0.43	4.5	74.0
	1.0	−343	121	220	0.31	3.2	81.4
50	Blank	−341	145	239	1.61	22.2	
	0.2	−343	139	241	1.33	14.0	36.8
	0.4	−339	136	236	1.10	11.2	49.5
	0.6	−338	138	233	0.92	9.4	57.6
	0.8	−340	134	231	0.65	6.7	69.7
	1.0	−342	128	227	0.54	5.55	74.9

barrier film formed on the metal surface reduces the probability of both the anodic and cathodic reactions. Thus, the inhibitor, ATPI, can be regarded as a mixed type inhibitor.

Electrochemical impedance spectroscopy (EIS) studies

Figure 2 shows the Nyquist plots for the corrosion of weld aged maraging steel in 1.5 M HCl solution at 45°C in the presence of different concentrations of ATPI. Similar plots were obtained at other temperatures also. The experimental results of EIS measurements obtained for the corrosion of weld aged maraging steel are summarized in Table 3.

As seen from Fig. 2 the Nyquist plots are semicircular in the presence as well as in the absence of inhibitor. This indicates that the corrosion of weld aged maraging steel is controlled by a charge transfer process and the addition of ATPI does not change the reaction mechanism of the corrosion of sample in HCl solution.[35] ATPI inhibits the corrosion primarily through its adsorption and subsequent formation of a barrier film on the metal surface.[36] This is in accordance with the observations of Tafel polarization measurements. It is seen from Fig. 2 that the Nyquist plots are not perfect semicircles. The deviation has been attributed to frequency dispersion, a phenomenon often corresponding with surface heterogeneity which may be the result of surface roughness, dislocations, distribution of the active sites, or adsorption of molecules.[37]

The data in Table 3 reveal that the charge transfer resistance (R_{ct}) increases with the increase in the inhibitor concentration, suggesting a hindrance to the charge transfer reaction (i.e., effective metal dissolution).[38] The increase in R_{ct} values is due to the gradual replacement of water molecules by the adsorption of the inhibitor molecules on the metal surface to form an adherent film on the metal surface and thereby reducing the metal dissolution in the solution. As R_{ct} is inversely proportional to the corrosion current density, inhibitor efficiency, η (%), was calculated from the following relationship:

$$\eta\,(\%) = \frac{R_{ct(inh)} - R_{ct}}{R_{ct(inh)}} \times 100 \qquad (3)$$

where $R_{ct(inh)}$ and R_{ct} are the charge transfer resistances obtained in inhibited and uninhibited solutions, respectively.

The corrosion current density i_{corr} can be calculated using the charge transfer resistance value, R_{ct}, using with the Stern–Geary equation (4).[39]

$$i_{corr} = \frac{b_a b_c}{2.303(b_a + b_c)R_{ct}} \qquad (4)$$

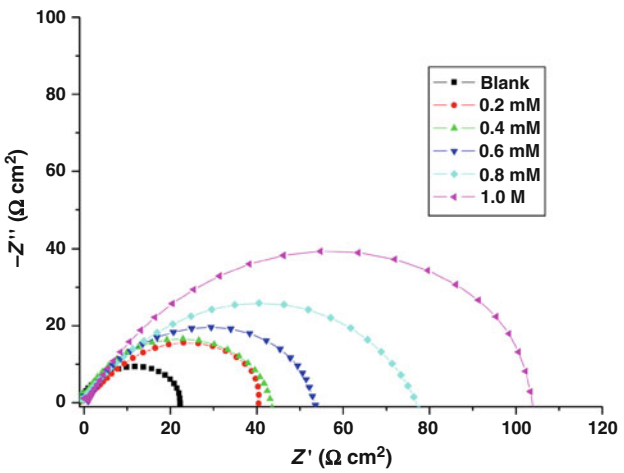

Fig. 2: Nyquist plots for the corrosion of weld aged maraging steel specimen in 1.5 M hydrochloric acid containing different concentrations of inhibitor at 45°C

Table 3: EIS data of weld aged maraging steel in 1.5 M hydrochloric acid containing different concentrations of ATPI

Temperature (°C)	Conc. of inhibitor (mM)	R_{ct} (Ω cm²)	C_{dl} (μF cm²)	η (%)
30	Blank	50	3028	
	0.2	88	1719	43.2
	0.4	121	1260	58.7
	0.6	156	573	68.0
	0.8	331	225	84.9
	1.0	418	197	88.0
35	Blank	45	3278	
	0.2	78	2317	42.0
	0.4	97	1825	53.6
	0.6	119	1377	62.2
	0.8	181	647	75.1
	1.0	258	403	82.6
40	Blank	43	4049	
	0.2	73	2364	41.0
	0.4	91	1952	52.7
	0.6	112	1745	61.6
	0.8	149	925	72.1
	1.0	219	869	81.3
45	Blank	24	4301	
	0.2	40	3498	40.0
	0.4	43	3235	44.1
	0.6	55	3049	54.7
	0.8	78	1597	67.5
	1.0	107	1194	76.1
50	Blank	25	4516	
	0.2	38	3946	34.2
	0.4	47	3756	46.8
	0.6	54	3451	53.7
	0.8	69	2715	63.7
	1.0	91	1938	72.5

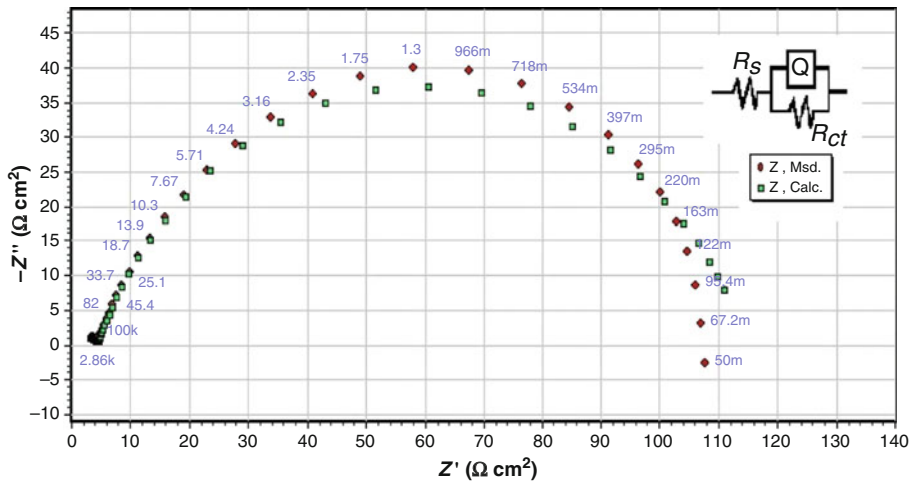

Fig. 3: Equivalent circuit used to fit the experimental EIS data for the corrosion of weld aged maraging steel specimen in hydrochloric acid at 45°C

The data in Table 3 also show that the value of C_{dl} decreases with the increase in the concentration of ATPI. This decrease in C_{dl} could be due to the decrease in the local dielectric constant and/or an increase in the thickness of the electrical double layer as a result of the adsorption of ATPI molecules at the electrochemical interface and thereby thickening of the electrical double layer.

The results obtained can be interpreted in terms of the equivalent circuit of the electrical double layer shown in Fig. 3 which has also been used previously to model the iron/acid interface.[40] The circuit fitment was done by ZSimpWin software version 3.21. The equivalent circuit (Fig. 3) is a parallel combination of the charge-transfer resistance (R_{ct}) and the constant phase element (CPE, Q), both in series with the solution resistance (R_s). The CPE element is used to explain the depression of the capacitance semicircle. The CPE impedance (Z_{CPE}) is given by the expression,

$$Z_{CPE} = \frac{1}{Q} \times \frac{1}{(j\omega)^n} \tag{5}$$

where Q is the CPE coefficient, n is the CPE exponent (phase shift), ω is the angular frequency ($\omega = 2\pi f$, where f is the AC frequency), and j is the imaginary unit. When the value of n is 1, the CPE behaves like an ideal double-layer capacitance (C_{dl}). The correction of capacity to its real values is calculated from

$$C_{dl} = Q(\omega_{max})^{n-1} \tag{6}$$

where ω_{max} is the frequency at which the imaginary part of impedance ($-Z_i$) has a maximum.[41]

Effect of temperature

The study on the effect of temperature on the corrosion rate and inhibition efficiency facilitates the calculation of kinetic and thermodynamic parameters for the inhibition and the adsorption processes. These parameters are useful in interpreting the type of adsorption by the inhibitor. The results in Tables 2 and 3 show that corrosion rate increases and the inhibition efficiency of ATPI decreases with the increase in temperature. The decrease in inhibition efficiency with the increase in temperature indicates desorption of the inhibitor molecules from the metal surface on increasing the temperature.[25] This fact is also suggestive of physisorption of the inhibitor molecules on the metal surface.

The value of activation energy (E_a) was calculated using the Arrhenius law equation,[42]

$$\ln(\upsilon_{corr}) = B - \frac{E_a}{RT} \tag{7}$$

where B is a constant which depends on the metal type, R is the universal gas constant, and T is the absolute temperature. The plot of $\ln(\upsilon_{corr})$ vs reciprocal of absolute temperature ($1/T$) gives a straight line with slope = $-E_a/R$, from which the activation energy values for the corrosion process were calculated. The Arrhenius plots for the corrosion of weld aged maraging steel in the presence of different concentrations of ATPI in 1.5 M hydrochloric acid are shown in Fig. 4.

The enthalpy and entropy of activation values for the corrosion process ($\Delta H^{\#}$ and $\Delta S^{\#}$) were calculated from transition state equation[8]

$$\upsilon_{corr} = \frac{RT}{Nh} \exp\left(\frac{\Delta S^{\#}}{R}\right) \exp\left(\frac{-\Delta H^{\#}}{R}\right) \tag{8}$$

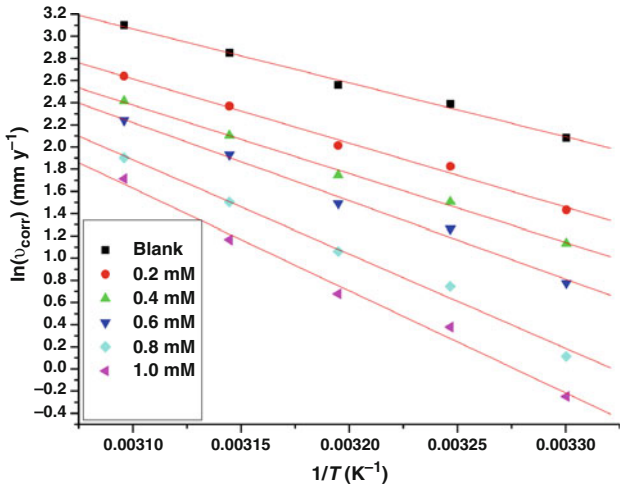

Fig. 4: Arrhenius plots for the corrosion of weld aged maraging steel in 1.5 M hydrochloric acid containing different concentrations of inhibitor

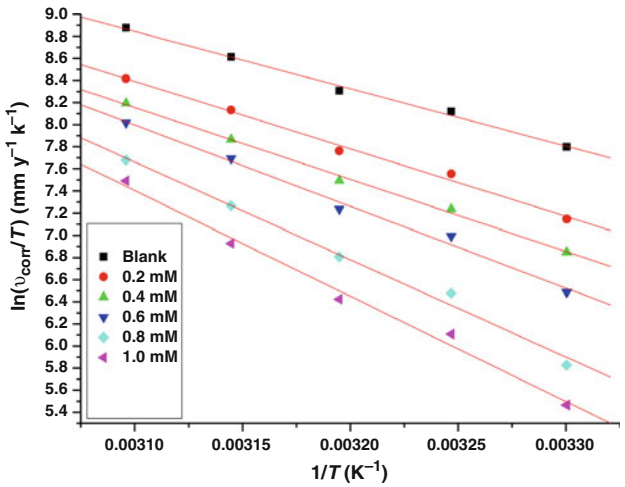

Fig. 5: Plots of ln(υ_{corr}/T) vs $1/T$ for the corrosion of weld aged maraging steel in 1.5 M hydrochloric acid containing different concentrations of inhibitor

where h is Plank's constant, and N is Avagadro's number. A plot of ln(υ_{corr}/T) vs $1/T$ gives a straight line with slope = $-\Delta H_a/T$ and intercept = ln(R/Nh) + $\Delta S_a/R$. The plots of ln(υ_{corr}/T) vs $1/T$ for the corrosion of weld aged samples of maraging steel in the presence of different concentrations of ATPI is shown in Fig. 5. The calculated values of activation parameters are recorded in Table 4. The results show that the value of E_a increases with the increase in the concentration of ATPI indicating that the energy barrier for the corrosion reaction increases. It is also indicated that the whole process is controlled by surface reaction,[3] since the activation energies of the corrosion process are above 20 kJ mol^{-1}. The adsorption of the inhibitor

Table 4: Activation parameters for the corrosion of weld aged maraging steel in 1.5 M hydrochloric acid containing different concentrations of inhibitor

Conc. of inhibitor (mM)	E_a (kJ mol^{-1})	$\Delta H^{\#}$ (kJ mol^{-1})	$\Delta S^{\#}$ (J mol^{-1} K^{-1})
Blank	40.55	43.12	−11.37
0.2	48.15	50.74	−29.79
0.4	51.42	53.97	−37.62
0.6	58.59	61.20	−58.58
0.8	70.61	73.22	−93.08
1.0	76.66	79.26	−109.62

on the electrode surface leads to the formation of a physical barrier between the metal surface and the corrosion medium, blocking the charge transfer, and thereby reducing the metal reactivity in the electrochemical reactions of corrosion. The decrease in the inhibition efficiency of ATPI with the increase in temperature can be considered to be because of the decrease in the extent of adsorption of the inhibitor on the metal surface with the increase in temperature, and corresponding increase in corrosion rate as a greater area of the metal surface is exposed to the corrosion medium. The observations also support the view that the inhibitor is adsorbed on the metal surface through physisorption.[25]

The entropy of activation values in the absence and the presence of ATPI are large and negative; this indicates that the activated complex formation in the rate-determining step represents an association rather than dissociation, decreasing the randomness on going from the reactants to the activated complex.[43] It is also seen from the table that entropy of activation decreases with the increase in the concentration of ATPI. This could be the result of the adsorption of the inhibitor molecules, which could be regarded as a quasi-substitution process between the inhibitor compound in the aqueous phase and water molecules at electrode surface. In the present case, the more orderly arrangement of the inhibitor molecules on the metal surface overweighs the solvent entropy resulting from desorption of water molecules from the metal surface.

Adsorption behavior

The adsorption of ATPI molecules on the metal surface can occur either through donor–acceptor interaction between the unshared electron pairs and/or π electrons of inhibitor molecule and the vacant d-orbitals of the metal surface atoms, or through electrostatic interaction of the inhibitor molecules with already adsorbed chloride ions.[34] The adsorption of an organic adsorbate on a metal solution interface can be represented as a substitution process between the organic molecules in the aqueous solution ($Org_{(sol)}$)

and the water molecules on the metallic surface ($H_2O_{(ads)}$)[25] as represented below:

$$Inh_{(sol)} + \chi H_2O_{(ads)} \leftrightarrow Org_{(ads)} + \chi H_2O_{(sol)} \quad (9)$$

where $Org_{(sol)}$ and $Org_{(ads)}$ are the organic molecules in the aqueous solution and adsorbed on the metallic surface, respectively; $H_2O_{(ads)}$ and $H_2O_{(sol)}$ are the water molecules on the metallic surface and in the solution, respectively; and χ represents the number of water molecules replaced by one molecule of organic adsorbate. Thus, in aqueous acidic solution, ATPI exists partly in the form of protonated species and partly as neutral molecules.[44]

The information on the interaction between the inhibitor molecules and the metal surface can be provided by adsorption isotherm. The degree of surface coverage (θ) for different concentrations of inhibitor was evaluated from potentiodynamic polarization measurements. The data were applied to various isotherms including Langmuir, Temkin, Frumkin and Flory–Huggins isotherms. It was found that the data fit best with the Langmuir adsorption isotherm according to which, the surface coverage (θ) is related to the inhibitor concentration C_{inh} by the following relation[25]:

$$\frac{C_{inh}}{\theta} = C_{inh} + \frac{1}{K} \quad (10)$$

where K is the adsorption/desorption equilibrium constant, C_{inh} is the corrosion inhibitor concentration in the solution, and θ is the surface coverage, which is calculated using equation (11)

$$\theta = \frac{\eta\,(\%)}{100} \quad (11)$$

where η (%) is the percentage inhibition efficiency as calculated using equation (1). The plot of C_{inh}/θ vs C_{inh} gives a straight line with an intercept of $1/K$. The Langmuir adsorption isotherms for the adsorption of ATPI on the maraging steel surface are shown in Fig. 6. The plots are linear, with correlation coefficients ranging from 0.9832 to 0.9929, with an average value of 0.9894. The slopes of the isotherms show deviation from the value of unity as would be expected for the ideal Langmuir adsorption isotherm equation. This deviation from unity may be due to the interaction among the adsorbed species on the metal surface. The Langmuir isotherm equation is based on the assumption that adsorbed molecules do not interact with one another, but this is not true in the case of organic molecules having polar atoms or groups which are adsorbed on the cathodic and anodic sites of the metal surface. Such adsorbed species may interact by mutual repulsion or attraction.

The values of standard free energy ΔG°_{ads} of adsorption are related to K by the relation shown in equation (12).[38]

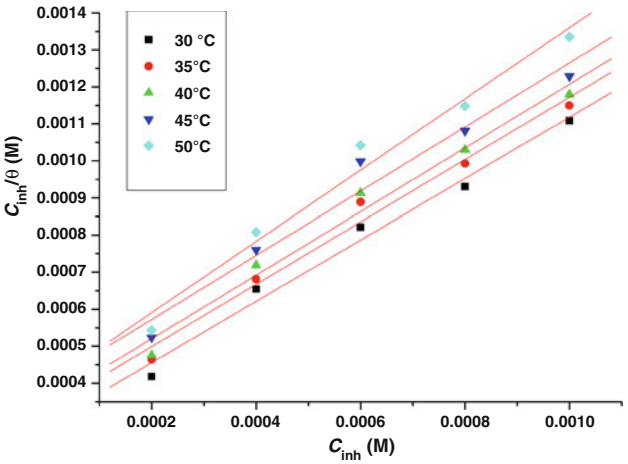

Fig. 6: Langmuir adsorption isotherms for the adsorption of ATPI on weld aged maraging steel in 1.5 M hydrochloric acid at different temperatures

Table 5: Thermodynamic parameters for the adsorption of ATPI on weld aged maraging steel surface in 1.5 M hydrochloric acid at different temperatures

Temperature (°C)	$-\Delta G^{\circ}_{ads}$ (kJ mol^{-1})	ΔH°_{ads} (kJ mol^{-1})	ΔS°_{ads} (J mol^{-1} K^{-1})
30	31.81		
35	31.31		
40	31.17	−49	−57
45	30.80		
50	30.63		

$$K = \frac{1}{55.5}\exp\left(\frac{-\Delta G^{\circ}_{ads}}{RT}\right) \quad (12)$$

where the value 55.5 is the concentration of water in solution in mol dm^{-3}, R is the universal gas constant, and T is absolute temperature. Standard enthalpy of adsorption (ΔH°_{ads}) and standard entropies of adsorption (ΔS°_{ads}) were obtained from the plot of (ΔG°_{ads}) vs T according to the thermodynamic equation (13).

$$\Delta G^{\circ}_{ads} = \Delta H^{\circ}_{ads} - T\Delta S^{\circ}_{ads} \quad (13)$$

The thermodynamic data obtained are tabulated in Table 5.

The negative values of ΔG°_{ads} indicate the spontaneity of the adsorption process and the stability of the adsorbed layer on the metal surface. Generally the values of ΔG°_{ads} less than −20 kJ mol^{-1} are consistent with physisorption, while those greater than −40 kJ mol^{-1} correspond to chemisorptions.[45] The calculated values of ΔG°_{ads} obtained in this study range between −31.81 and −30.64 kJ mol^{-1}, indicating both physical and chemical adsorption behaviors of ATPI on the metal surface.[46]

The negative sign of ΔH°_{ads} in HCl solution indicates that the adsorption of inhibitor molecules is an exothermic process. Generally, an exothermic adsorption process signifies either physisorption or chemisorptions while the endothermic process is attributable unequivocally to chemisorption. Typically, the standard enthalpy of the physisorption process is less negative than 41.86 kJ mol^{-1}, while that of the chemisorptions process approaches -100 kJ mol^{-1}. In the present study, the value of ΔH°_{ads} is -49 kJ mol^{-1} which shows that the adsorption of ATPI on weld aged maraging steel involves both physisorption and chemisorption phenomena. From the thermodynamic data and also from the variation of corrosion inhibition efficiency with temperature it can be concluded that the ATPI gets adsorbed on the metal surface through both physisorption and chemisorption, but physisorption is more predominant. The predominant physical adsorption is also inconsistent with the decrease in inhibition efficiency and with the increase in temperature. The ΔS°_{ads} value is large and negative, indicating that an ordering takes place when the inhibitor gets adsorbed on the metal alloy surface.[17]

Inhibition mechanism

Inhibitive action of ATPI on the corrosion of weld aged maraging steel in acidic solutions can be explained on the basis of adsorption. The adsorption of ATPI molecules on the metal surface can be attributed to the presence of electronegative elements like nitrogen and sulfur and also to the presence of π electron cloud in the benzene ring of the molecule. TPI inhibits the corrosion by controlling both the anodic and cathodic reactions.

In HCl solution, the following mechanism is proposed for the corrosion of iron and steel.[47] According to this mechanism anodic dissolution of iron takes place as follows:

$$Fe + Cl^{-} \rightarrow (FeCl^{-})_{ads} \quad (14)$$

$$(FeCl^{-})_{ads} \rightarrow (FeCl)_{ads} + e^{-} \quad (15)$$

$$(FeCl)_{ads} \rightarrow (FeCl^{+})_{ads} + e^{-} \quad (16)$$

$$(FeCl^{+})_{ads} \rightarrow Fe^{2+} + Cl^{-} \quad (17)$$

The nickel present in the maraging steel also undergoes anodic dissolution as follows[48]:

$$Ni + Cl^{-} \rightarrow (NiCl^{-})_{ads} \quad (18)$$

$$(NiCl^{-})_{ads} \rightarrow (NiCl)_{ads} + e^{-} \quad (19)$$

$$(NiCl)_{ads} \rightarrow (NiCl^{+})_{ads} + e^{-} \quad (20)$$

$$(NiCl^{+})_{ads} \rightarrow Ni^{2+} + Cl^{-} \quad (21)$$

In a cathodic reaction, hydrogen evolution takes place as follows:

$$Fe + H^{+} \rightarrow (FeH^{+})_{ads} \quad (22)$$

$$(FeH^{+})_{ads} + e^{-} \rightarrow (FeH)_{ads} \quad (23)$$

$$(FeH)_{ads} + H^{+} + e^{-} \rightarrow Fe + H_2 \quad (24)$$

In a highly acidic solution, as in the present case, the ATPI molecule can undergo protonation at its amino group and can exist as a protonated positive species. The protonated species gets adsorbed on the cathodic sites of the metal surface through electrostatic interaction, thereby decreasing the rate of the cathodic reaction. The presence of anions in the solution and their adsorption on the metal surface play an important role in the mechanism of inhibition exhibited by the organic compounds.[49] In a highly acidic medium like the one in the present investigation, the metal surface is positively charged. This would cause the negatively charged chloride ions to become adsorbed on the metal surface, making the metal surface negatively charged. The positively charged protonated ATPI molecules can interact electrostatically with the negatively charged chloride adsorbed metal surface, resulting in physisorption. The negative charge centers of the ATPI molecules containing a lone pair of electrons and/or π electrons can electrostatically interact with the anodic sites on the metal surface and get adsorbed. The neutral inhibitor molecules may occupy the vacant adsorption sites on the metal surface through the chemisorption mode involving the displacement of water molecules from the metal surface and sharing of electrons by the hetero atoms like nitrogen and/or sulphur with iron. Chemisorption is also possible by the donor–acceptor interactions between π electrons of the aromatic ring and the vacant d orbitals of iron, providing another mode of protection.[50] The presence of ATPI in the protonated form and the presence of negative charge centers on the molecule are also responsible for the mutual interaction of inhibitor molecules on the alloy surface. This is reflected in the deviation of slopes of Langmuir adsorption isotherms as discussed in the previous section.

Scanning electron microscopy

The effect of corrosion on the surface morphology of the maraging steel sample was assessed by recording the SEM images of the alloy samples subjected to corrosion in 1.5 M hydrochloric acid for 3 h in the presence and the absence of ATPI. Figure 7 shows the SEM images of the maraging steel sample. Figure 7a shows the facets due to the attack of hydrochloric acid on the metal surface with cracks and rough surfaces. Figure 7b shows the SEM image of the sample after immersion in 1.5 M hydrochloric acid in the presence

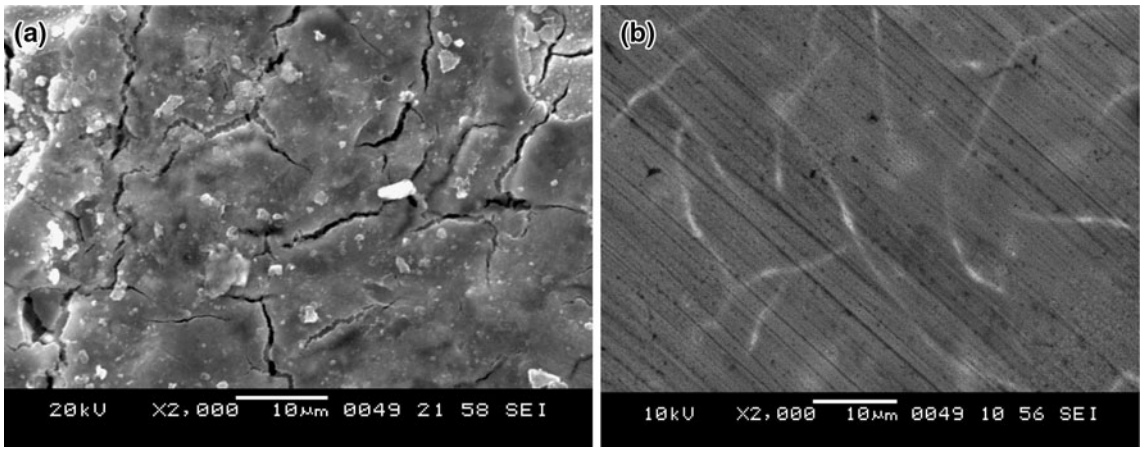

Fig. 7: SEM images of the weld aged maraging steel after immersion in 1.5 M hydrochloric acid (a) in the absence and (b) in the presence of ATPI

of ATPI. It can be seen that the alloy surface is smooth without any visible corrosion attack. Thus, it can be concluded that ATPI protects the alloy from corrosion by forming a uniform film on the alloy surface.

Conclusions

Based on the results of investigation, the following conclusions are drawn:

1. ATPI acts as a good inhibitor for the corrosion of weld aged maraging steel in 1.5 M HCl.
2. The inhibition efficiency increases with the increase in inhibitor concentration.
3. The inhibition efficiency of ATPI decreases with the increases in temperature.
4. The adsorption of ATPI obeys the Langmuir adsorption isotherm.
5. Values of standard enthalpy of adsorption and standard free energy of adsorption indicate that the adsorption of ATPI on the surface of weld aged maraging steel involves both physical and chemical processes.
6. ATPI acts as a mixed inhibitor by inhibiting both the anodic and cathodic reactions.
7. The results obtained from Tafel polarization studies and EIS studies are in a good agreement.

References

1. Ekpe, UJ, Ibok, UJ, Ita, BI, Offiong, OE, Ebenso, EE, ''Inhibitory Action of Methyl and Phenyl Thiosemicarbazone Derivatives on the Corrosion of Mild Steel in Hydrochloric Acid.'' *Mater. Chem. Phys.*, **40** 87–93 (1995)
2. Maayta, AK, Al-Rawashdeh, NAF, ''Inhibition of Acidic Corrosion of Pure Aluminum by Some Organic Compounds.'' *Corros. Sci.*, **46** 1129–1140 (2004)
3. Fouda, AS, Heakal, FE, Radwan, MS, ''Role of Some Thiadiazole Derivatives as Inhibitors for the Corrosion of C-Steel in 1 M H_2SO_4.'' *J. Appl. Electrochem.*, **39** 391–402 (2009)
4. Quraishi, MA, Sardar, R, ''Hector Bases—A New Class of Heterocyclic Corrosion Inhibitors for Mild Steel in Acid Solutions.'' *J. Appl. Electrochem.*, **33** 1163–1168 (2003)
5. Bentiss, F, Lebrini, M, Lagrenee, M, ''Thermodynamic Characterization of Metal Dissolution and Inhibitor Process in Mild Steel/2,5-Bis(*n*-thienyl)-1,3,4-thiadiazoles/Hydrochloric Acid System.'' *Corros. Sci.*, **47** 2915–2931 (2005)
6. Khaled, KF, Babic-Samardzija, K, Hackerman, N, ''Piperidines as Corrosion Inhibitors for Iron in HCl.'' *J. Appl. Electrochem.*, **34** 697–704 (2004)
7. Wang, H, Liu, RB, Xin, J, ''Inhibiting Effects of Some Mercapto-triazole Derivatives on the Corrosion of Mild Steel in 1.0 M HCl Medium.'' *Corros. Sci.*, **46** 2455–2466 (2004)
8. Abd El-Rehim, SS, Ibrahim, MAM, Khaled, KF, ''4-Aminoantipyrine as an Inhibitor of Mild Steel Corrosion in HCl Solution.'' *J. Appl. Electrochem.*, **29** 593–599 (1999)
9. Quraishi, MA, Jamal, D, ''Inhibition of Mild Steel Corrosion in the Presence of Fatty Acid Triazoles.'' *J. Appl. Electrochem.*, **32** 425–430 (2002)
10. Barouni, K, Bazzi, L, Salghi, R, Mihit, M, Hammouti, B, Albourine, A, El Issami, S, ''Some Amino Acids as Corrosion Inhibitors for Copper in Nitric Acid Solution.'' *Mater. Lett.*, **62** 3325–3327 (2008)
11. El Azhar, M, Mernari, B, Traisnel, M, Bentiss, F, Lagrenee, M, ''Corrosion Inhibition of Mild Steel by the New Class of Inhibitors [2,5-Bis(*n*-pyridyl)-1,3,4-thiadiazoles] in Acidic Media.'' *Corros. Sci.*, **43** 2229–2238 (2001)
12. Popova, A, Christov, M, Raicheva, S, Sokolova, E, ''Adsorption and Inhibitive Properties of Benzimidazole Derivatives in Acid Mild Steel Corrosion.'' *Corros. Sci.*, **46** 1333–1350 (2004)
13. Morad, MS, Kamal El-Dean, AM, ''2,2′-Dithiobis(3-cyano-4,6-dimethylpyridine): A New Class of Acid Corrosion Inhibitors for Mild Steel.'' *Corros. Sci.*, **48** 3398–3412 (2006)
14. Razek, J, Klein, IE, Yahalom, J, ''Structure and Corrosion Resistance of Oxides Grown on Maraging Steel in Steam at Elevated Temperatures.'' *Appl. Surf. Sci.*, **108** 159–167 (1997)
15. Ohue, Y, Matsumoto, K, ''Sliding–Rolling Contact Fatigue and Wear of Maraging Steel Roller with Ion-Nitriding and Fine Particle Shot-Peening.'' *Wear*, **263** 782–789 (2007)

16. Wang, W, Yan, W, Duan, Q, Shan, Y, Zhang, Z, Yang, K, ''Study on Fatigue Property of a New 2.8 GPa Grade Maraging Steel.'' *Mater. Sci. Eng. A*, **527** 3057–3063 (2010)
17. Poornima, T, Nayak, J, Shetty, AN, ''Corrosion of Aged and Annealed 18 Ni 250 Grade Maraging Steel in Phosphoric Acid Medium.'' *Int. J. Electrochem. Sci.*, **5** 56–71 (2010)
18. Stiller, K, Danoix, F, Bostel, A, ''Investigation of Precipitation in a New Maraging Stainless Steel.'' *Appl. Surf. Sci.*, **94** 326–333 (1996)
19. Klobcar, D, Tusek, J, Taljat, B, Kosec, L, Pleterski, M, ''Aging of Maraging Steel Welds During Aluminum Alloy Die Casting.'' *Mater. Sci.*, **44** 515–522 (2008)
20. Grum, J, Slabe, JM, ''Effect of Laser-Remelting of Surface Cracks on Microstructure and Residual Stresses in 12Ni Maraging Steel.'' *Appl. Surf. Sci.*, **252** 4486–4492 (2006)
21. Bellanger, G, Rameau, JJ, ''Effect of Slightly Acid pH With or Without Chloride in Radioactive Water on the Corrosion of Maraging Steel.'' *J. Nucl. Mater.*, **228** 24–37 (1996)
22. Bellanger, G, ''Effect of Carbonate in Slightly Alkaline Medium on the Corrosion of Maraging Steel.'' *J. Nucl. Mater.*, **217** 187–193 (1994)
23. Rezek, J, Klein, IE, Yhalom, J, ''Electrochemical Properties of Protective Coatings on Maraging Steel.'' *Corros. Sci.*, **39** 385–397 (1997)
24. Poornima, T, Jagannatha, N, Nityananda, AN, ''Studies on Corrosion of Annealed and Aged 18 Ni 250 Grade Maraging Steel in Sulphuric Acid Medium.'' *Portugal. Electrochim. Acta*, **28** 173–188 (2010)
25. Poornima, T, Nayak, J, Shetty, AN, ''3,4-Dimethoxy Benzaldehyde thiosemicarbazone as Corrosion Inhibitor for Aged 18Ni 250 Grade Maraging Steel in 0.5 M Sulfuric Acid.'' *J. Appl. Electrochem.*, **41** 223–233 (2011)
26. Gao, J, Weng, Y, Salitanat, Feng, L, Yue, H, ''Corrosion Inhibition of α, β-unsaturated Carbonyl Compounds on Steel in Acid Medium.'' *Pet. Sci.*, **6** 201–207 (2009)
27. Selim, IZ, Khedr, AA, El-Shobki, KM, ''Efficiency of Chalcone Compounds Inhibitors for Acid Corrosion of Al and Al-3.5 Mg Alloy.'' *J. Mater. Sci. Technol.*, **12** 267–272 (1996)
28. Hoong-Kun, F, Thawanrat, K, Suchada, C, ''(2E)-1-(4-Aminophenyl)-3-(2-thienyl)prop-2-en-1-one Ethanol Hemisolvate.'' *Acta Crystallogr. E*, **65** 2532–2533 (2009)
29. Fontana, MG, *Corrosion Engineering*, 3rd ed. McGraw- Hill, Singapore, 1987
30. Li, WH, He, Q, Pei, CL, Hou, BR, ''Experimental and Theoretical Investigation of the Adsorption Behavior of New Triazole Derivatives as Inhibitors for Mild Steel Corrosion in Acid Media.'' *Electrochim. Acta*, **52** 6386–6394 (2007)
31. Ferreira, ES, Giacomelli, C, Giacomelli, FC, Spinelli, A, ''Evaluation of the Inhibitor Effect of L-Ascorbic Acid on the Corrosion of Mild Steel.'' *Mater. Chem. Phys.*, **83** 129–134 (2004)
32. Li, WH, He, Q, Pei, CL, Hou, BR, ''Some New Triazole Derivatives as Inhibitors for Mild Steel Corrosion in Acidic Medium.'' *J. Appl. Electrochem.*, **38** 289–295 (2008)
33. Ehteshamzadeh, M, Jafari, AH, Naderi, E, Hosseini, MG, ''Effect of Carbon Steel Microstructure and Molecular Structure of Two New Schiff Base Compounds on Inhibition Performance in 1 N HCl Solution by EIS.'' *Mater. Chem. Phys.*, **113** 986–993 (2009)
34. Ateya, BG, El-Khair, MBA, Abdel-Hamed, IA, ''Thiosemicarbazide as an Inhibitor for the Acid Corrosion of Iron.'' *Corros. Sci.*, **16** 163–169 (1976)
35. Larabi, L, Harek, Y, Benali, O, Ghalem, S, ''Hydrazide Derivatives as Corrosion Inhibitors for Mild Steel in 1 M HCl.'' *Prog. Org. Coat.*, **54** 256–262 (2005)
36. Amin, MA, Abd El-Rehim, SS, El-Sherbini, EEF, Bayyomi, RS, ''The Inhibition of Low Carbon Steel Corrosion in Hydrochloric Acid Solutions by Succinic Acid: Part I. Weight Loss, Polarization, EIS, PZC, EDX and SEM Studies.'' *Electrochim. Acta*, **52** 3588–3600 (2007)
37. El Hosary, AA, Saleh, RM, Shams El Din, AM, ''Corrosion Inhibition by Naturally Occurring Substances. I. The Effect of Hibiscus Subdariffa (Karkade) Extract on the Dissolution of Al and Zn.'' *Corros. Sci.*, **12** 897–904 (1972)
38. Sanaa, TA, ''Inhibition Action of Thiosemicabazone and Some of it is ρ-Substituted Compounds on the Corrosion of Iron-base Metallic Glass Alloy in 0.5 M H_2SO_4 at 30°C.'' *Mater. Res. Bull.*, **43** 510–521 (2008)
39. El-Sayed, A, ''Phenothiazine as Inhibitor of the Corrosion of Cadmium in Acidic Solutions.'' *J. Appl. Electrochem.*, **27** 193–200 (1997)
40. Prabhu, RA, Venkatesha, TV, Shanbhag, AV, Kulkarni, GM, Kalkhambkar, RG, ''Inhibition Effects of Some Schiff's Bases on the Corrosion of Mild Steel in Hydrochloric Acid Solution.'' *Corros. Sci.*, **50** 3356–3362 (2008)
41. Machnikova, E, Kenton Whitmire, H, Hackerman, N, ''Corrosion Inhibition of Carbon Steel in Hydrochloric Acid by Furan Derivatives.'' *Electrochim. Acta*, **53** 6024–6032 (2008)
42. Bouklah, M, Hammouti, B, Aounti, A, Benhadda, T, ''Thiophene Derivatives as Effective Inhibitors for the Corrosion of Steel in 0.5 M H_2SO_4.'' *Prog. Org. Coat.*, **49** 227–236 (2004)
43. Abd EI Rehim, SS, Hassan, HH, Amin, MA, ''The Corrosion Inhibition Study of Sodium Dodecyl Benzene Sulphonate to Aluminium and Its Alloys in 1.0 M HCl Solution.'' *Mater. Chem. Phys.*, **78** 337–348 (2003)
44. Oguzie, EE, Njoku, VO, Enenebeak, CK, Akalezi, CO, Obi, C, ''Effect of Hexamethylpararosaniline Chloride (Crystal Violet) on Mild Steel Corrosion in Acidic Media.'' *Corros. Sci.*, **50** 3480–3486 (2008)
45. Fuchs, GR, ''The Adsorption, CMC Determination and Corrosion Inhibition of Some *N*-Aalkyl Quaternary Ammonium Salts on Carbon Steel Surface in 2 M H_2SO_4.'' *Colloids Surf. A*, **280** 130–138 (2006)
46. Hosseini, M, Mertens, SFL, Arshadi, MR, ''Synergism and Antagonism in Mild Steel Corrosion Inhibition by Sodium Dodecyl Benzenesulphonate and Hexamethylenetetramine.'' *Corros. Sci.*, **45** 1473–1482 (2003)
47. Ashish Kumar, S, Quraishi, MA, ''Effect of Cefazolin on the Corrosion of Mild Steel in HCl Solution.'' *Corros. Sci.*, **52** 152–160 (2010)
48. Burstein, G, Wright, G, ''The Anodic Dissolution of Nickel-II. Bromide and Iodide Electrolytes.'' *Electrochim. Acta*, **21** 311–314 (1976)
49. Hackerman, N, Snavely, ES, Jr, Payne, JS, Jr, ''Effects of Anions on Corrosion Inhibition by Organic Compounds.'' *J. Electrochem. Soc.*, **113** 677–686 (1966)
50. Satpati, AK, Ravindran, PV, ''Electrochemical Study of the Inhibition of Corrosion of Stainless Steel by 1,2,3-Benzotriazole in Acidic Media.'' *Mater. Chem. Phys.*, **109** 352–359 (2008)